RAPID COMMUNICATIONS

PHYSICAL REVIEW B **80**, 220103(R) (2009)

# Three-dimensional random-field Ising model phase transition in virgin $Sr_{0.4}Ba_{0.6}Nb_2O_6$: Overcoming aging

S. Miga,[1] W. Kleemann,[2,*] J. Dec,[3] and T. Łukasiewicz[4]
[1]*Institute of Physics, University of Silesia, PL 40-007 Katowice, Poland*
[2]*Angewandte Physik, Universität Duisburg-Essen, D 47048 Duisburg, Germany*
[3]*Institute of Materials Science, University of Silesia, PL 40-007 Katowice, Poland*
[4]*Institute of Electronic Materials Technology, PL 01-919 Warsaw, Poland*
(Received 16 November 2009; published 11 December 2009)

Isothermal aging above the ferroelectric phase-transition temperature, $T_c \approx 410$ K, causes the charge-disordered uniaxial crystal $Sr_{0.40}Ba_{0.60}Nb_2O_6$ to become trapped in metastable nanopolar states at any finite wait time. However, backward extrapolation of the isothermal relaxation of its axial linear susceptibility $\chi'$ under various frequency, time, and temperature protocols allows disclosing its unaged virgin state. In this limit it is supposed to undergo a sharp weakly first-order transition within the framework of the three-dimensional random-field Ising model.

DOI: 10.1103/PhysRevB.80.220103 PACS number(s): 64.60.De, 77.22.Ch, 77.80.Bh, 77.84.Dy

Aging is a widespread phenomenon in disordered systems such as spin or orientational glasses, supercooled liquids, polymers, and relaxor ferroelectrics.[1] It is a distinct experimental consequence of their nonequilibrium state even on macroscopic time scales and is most readily identified by checking the ac susceptibility on cooling rates, wait times, and temperature variations. Very often it is related to the growth of "domains" or "droplets" in the initial metastable state toward the long-range order of the respective ground state. Different scenarios such as cumulative aging as in glassy poly(methylmethacrylate)[2] or imprint of a "holelike memory" accompanied by "rejuvenation" effects as in spin glasses[3] are meanwhile reasonably well understood.[1]

Comparatively ill-understood systems with aging tendencies refer to the random-field Ising model (RFIM). It is expected to undergo a sharp phase transition into the long-range order in the weak RF limit[4] provided that the extremely slow critical relaxation[5] can be overcome on cooling to below the transition temperature $T_c$. Otherwise, the system impends to decay into domains, which will blur criticality. Promising candidates for achieving this goal are dilute uniaxial antiferromagnets in a uniform magnetic field (DAFF).[6] However, even after zero-field cooling (ZFC) to below $T_c$ and subsequent application of the field they have left open questions about the asymptotic critical behavior.[7] For example, in $Fe_{0.85}Zn_{0.15}F_2$, despite extremely slow temperature scans the x-ray scattering intensity at antiferromagnetic Bragg spots suffers from thermal hysteresis, hence indicating nonequilibrium behavior in the vicinity of the supposed transition temperature, $T_N \approx 63$ K.[8]

Similar mysterious behavior characterizes the ferroic RFIM system, the ferroelectric uniaxial relaxor crystal $Sr_{0.61}Ba_{0.39}Nb_2O_6$ (SBN61).[9] It fails to show the expected critical behavior since it gets unavoidably stuck in a frozen polar nanodomain state when approaching the Curie temperature, $T_c \approx 345$ K,[10] even at extremely slow cooling rates. As a consequence, the observed criticality was proposed to be merely due to the quasi-two-dimensional (2D) interfaces between the nanodomains, in accordance with the observed set of 2D Ising model critical exponents, $\alpha \approx 0$, $\beta \approx 1/8$, and $\gamma \approx 7/4$.[11]

Indeed, polar nanoregions have very clearly been observed in SBN40, 50, 61, and 75 above $T_c$ by scanning piezoelectric force microscopy (PFM).[12] By employing a time-dependent stochastic field equation method, Semenovskaya and Khachaturyan[13] were able to calculate the evolution of quasistable polar regions (domains) due to the fluctuations of the random field of static defects within the paraelectric phase of a ferroelectric system. The electrostatic dipole-dipole interaction between domains and phases proved to be a decisive additional ingredient. The "mixed phase" was shown to lose ergodicity, i.e., becoming path dependent and to resemble a glasslike situation.

In order to circumvent this bottleneck we abandoned the strong random fields of relaxorlike SBN61 and examined crystals with lower $Sr^{2+}$ contents like $Sr_{0.40}Ba_{0.60}Nb_2O_6$ (SBN40). It has a lower effective charge disorder—the very origin of random fields in SBN (Ref. 9)—and avoids the relaxor-typical frequency-dependent high-$T$ shift of the susceptibility peak $T_m$.[12] Similar considerations once caused to shift the focus of interest from high to low diamagnetic dilutions in DAFF materials.[8]

In this Rapid Communication we confirm, indeed, the reduction in some relaxor-typical signatures in SBN40; however, nonergodicity is still indicated by the appearance of substantial aging of the real part of the susceptibility with wait time, $\chi'(\Delta t)$. The isothermal decay obeys stretched exponential temporal behavior, which allows one to extrapolate the response back to the unaged "virgin" state at $\Delta t = -t_0$. We argue that this signal corresponds to the "pure" RFIM response, which becomes unscreened by polar cluster formation only in the limit $\Delta t \to -t_0$. As a consequence, the weakly first-order transition in SBN40 appears sharp in the absence of interfaces as predicted by Imry and Wortis.[14] At finite aging times, irreversible domains appear[13] and create metastability even above the phase-transition temperature.[11] We claim that previous attempts to verify three-dimensional (3D) RFIM criticality in SBN (Refs. 9 and 11) and probably also in DAFF (Ref. 8) have failed due to the loss of generic randomness after "equilibrating" the samples into domain states via unavoidable irreversible aging.

 

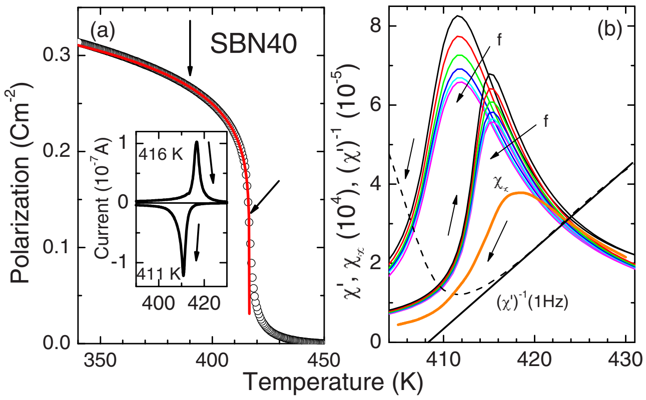


FIG. 1. (Color online) (a) Polarization decay on zero-field heating (after field cooling), $P$ vs $T$, at the phase transition of SBN40 fitted for the $T$ values between arrows by a critical power law ( solid line). Thermal hysteresis is revealed (a) between FC-ZFH and ZFC polarization currents (inset) and (b) in the real part of the linear susceptibility, $\chi'$ vs $T$, recorded with $f=10^0-10^5$ Hz at rates $\pm0.1$ K min$^{-1}$ on cooling and heating in zero field (arrows). The infinitely aged response on cooling, $\chi_\infty(f=37\text{ Hz})$ [see Eq. (1) and Fig. 2(b)], and $(\chi')^{-1}(f=1\text{ Hz})$ on cooling (dashed line) with an inverse Curie-Weiss fit (solid straight line) are shown for comparison.

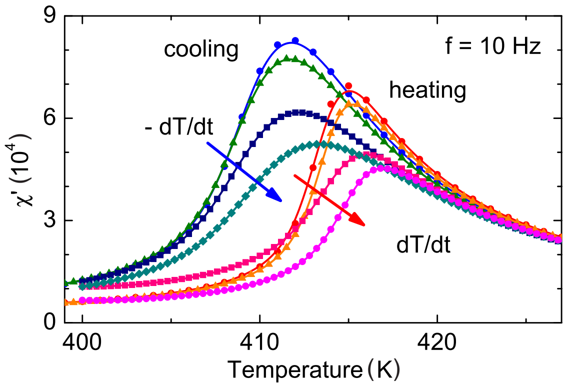


FIG. 2. (Color online) Thermal hysteresis between FC-ZFH and ZFC susceptibility curves, $\chi'$ vs $T$, recorded at $f=10$ Hz at heating and cooling rates, $|dT/dt|=0.012$, 0.035, 0.1, and 0.2 K min$^{-1}$ (arrows).

The SBN40 single crystals used in this study were grown by the Czochralski method[15] and cut into platelet-shaped samples of size $5\times5\times0.5$ mm$^3$ perpendicular to the polar $c$ axis (=crystallographic direction [001]). The polarization was calculated by integrating the pyroelectric current measured with a Stanford Research SR 570 current preamplifier during zero-field heating (ZFH) after field cooling (FC). The dielectric susceptibility, $\chi=\chi'-i\chi''$, was measured with either a Solartron 1260 impedance analyzer and 1296 dielectric interface or a homebuilt impedance analyzer[16] at ac probing field amplitudes $E_0\approx500$ V/m and frequencies $10^0\leq f\leq10^5$ Hz. Temperatures were controlled to within $\pm0.005$ K using a Lake Shore 340 temperature controller.

The inset of Fig. 1(a) shows the pyroelectric currents on ZFH (upper curve) after FC the sample at $E\approx3.6$ kV/m and subsequently on ZFC (lower curve). They are peaking with magnitudes of $\approx10^{-7}$ A and a sizable thermal hysteresis at 416 ($\leq T_1$) and 411 K ($\geq T_0$), respectively.[17] Although $P$ vs $T$ [Fig. 1(a), main panel] has a concave tail up to $\approx435$ K, one encounters a fairly sharp drop at the transition temperature. A best fit within $390\leq T\leq406$ K (arrows) to a power law, $P\propto(T^*-T)^{-\beta}$, yields $T^*=416.5\pm0.1$ K ($\leq T_1$) and $\beta=0.14\pm0.01$. The exponent comes close to that reported previously for SBN61 (Ref. 9) and discussed subsequently[11] in terms of 2D Ising criticality. Note, however, that the observed thermal hysteresis clearly indicates a first-order transition and the apparent criticality has probably to be interpreted as a smeared discontinuity.[14]

This is corroborated by axial ac susceptibility data shown in Fig. 1(b) for frequencies $10^0\leq f=\omega/2\pi\leq10^5$ Hz both on heating and cooling (arrows). Despite the very slow rates, $\pm0.1$ K min$^{-1}$, distinct peaks appear invariably at $T_m\approx415$ and 412 K, respectively. In contrast to systems with higher $Sr^{2+}$ content, e.g., SBN61,[9,12] their positions virtually do not depend on $f$, while the amplitude decreases by $\approx20\%$ when increasing the frequency by five orders of magnitude. Similarly, as shown in Fig. 2, the hysteresis width is virtually independent of the cooling and heating rates, respectively, within the range $0.01\leq|dT/dt|\leq0.2$ K min$^{-1}$, while the amplitudes decrease by $\approx35\%$ at increasing rates in the same interval. Hence, it can be safely excluded that the hysteresis shrinks to zero at infinitely slow rates thus corroborating the first-order nature of the transition. Here, we notice that a first-order scenario[14] does not contradict the basic ideas of the RFIM, which was originally considered for a second-order phase transition.[4]

The inverse susceptibility at $T>T_m+6$ K (on cooling) obeys a Curie-Weiss thermal behavior, $(\chi')^{-1}\propto T-T_0$ with $T_0\approx408.5$ K,[17] while rounding occurs within $T\approx T_m\pm6$ K as shown for the cooling curve at $f=1$ Hz in Fig. 1(b). Hence, beyond the mean-field regime only appreciable smearing—obviously due to a wide distribution of transition temperatures—is encountered. The shape of the susceptibility curves is, however, not temporally stable. The irreversible aging of the dielectric permittivity was previously shown on SBN61 in its ferroelectric domain state,[18] and even in its paraelectric regime, $T>330$ K.[10] Inspection showed that the decrease follows a stretched exponential decay law, which is typical of hierarchical growth processes.[19] It was attributed to irreversible growth of mesoscopic polar nanoregions, which optimize their local free energy while decreasing their total interface area and, hence, decrease both $\chi'$ and $\chi''$. We have studied this behavior on SBN40 in more detail and show some examples in Fig. 3(a). After cooling at the rate $dT/dt=-0.04$ K/s from the common start (and refresh) temperature, $T_r=470$ K, to 26 final temperatures within $403\leq T\leq430$ K, $\chi'$ was measured at $f=37$, 111, 334, 1000, and 3000 Hz. The resulting decay curves were then fitted to a time-shifted stretched exponential function[19]

$$\chi'(\omega,\Delta t)=\Delta\chi(\omega)\exp[-\{(\Delta t+t_0)/\tau\}^{\beta}]+\chi_\infty(\omega),\qquad(1)$$

where $\Delta t$ is the wait time. Equation (1) involves five fit parameters: (a) the decaying amplitude $\Delta\chi(\omega)$, (b) the microscopic relaxation time $\tau$, (c) the stretching exponent $\beta$ ac-

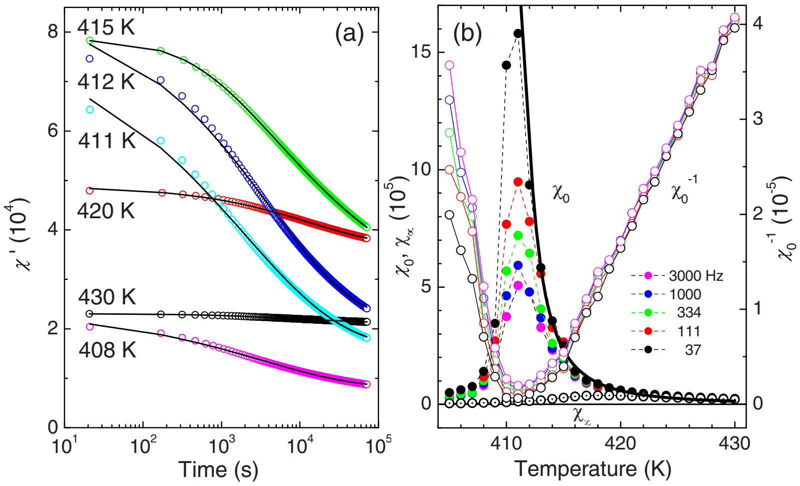


FIG. 3. (Color online) (a) Temporal relaxation of the linear susceptibility, $\chi'(f=10^3\ \text{Hz})$, recorded after ZFC to various constant temperatures and fitted to Eq. (1) (solid lines). Only selected curves are shown. (b) Asymptotic values $\chi_\infty$, $\chi_0$, and $\chi_0^{-1}$ vs $T$ (center dot, solid, and open circles, respectively) obtained for five different frequencies $f$ and 26 aging temperatures $T$ together with a power-law fit of $\chi_0(f=37\ \text{Hz})$ vs $T$ (bold solid line).

counting for the finite width of the relaxation time distribution, (d) an extrapolated aging time $t_0$ to be added to the experimental start time $\Delta t$ (it is negligibly small when describing the aging of the ferroelectric domain state[18]), and (e) a time-invariant contribution to the permittivity $\chi_\infty(\omega)$. Note that this latter ansatz assumes that all dynamic and asymptotic contributions [first and second terms in Eq. (1), respectively] are preformed from the beginning, thus completely describing the birth of the nanoregions at $\Delta t \geq -t_0$ and their transformation into polar domains as $\Delta t \to \infty$ (see the inset in Fig. 4). Indeed, in view of the smooth crossover into the aged response, $\chi_\infty(\omega)$ [see below; Fig. 3(b)], qualitatively new features do not occur. High-quality fits to the data are shown in Fig. 3(a) and corroborate the adequacy of Eq. (1).

Figure 4 shows the resulting best-fit parameters $\tau$, $t_0$, and $\beta$ for all 26 aging temperatures $T$ and the above five frequencies $f$. It is seen that the microscopic relaxation time becomes shortest, $\tau < 10^{-4}$ s, in the vicinity of the transition temperature, $T_0 \approx 410$ K, while it reaches large values, $20 < \tau < 7000$ s, at $|T-T_0| > 5$ K. In parallel, very small stretching exponents, $\beta \approx 0.1$, and hence very wide distributions of relaxation times characterize the "critical" region, $|T-T_0| < 5$ K, while moderate stretching with $\beta \approx 0.3$ occurs far distant from $T_0$. The parallel trends of both $\tau$ and $\beta$ give rise to fairly constant autocorrelation times,[20] $\langle\tau\rangle = (\tau/\beta)\Gamma(1/\beta) \approx 10^3, \ldots, 10^4$ s (not shown), where $\Gamma(x)$ denotes the gamma function. The best-fitted virtual starting times from the unaged state, $-t_0 \approx -200, \ldots, -900$ s (Fig. 4), are compatible with the experimental cooling times. This is corroborated for increasing cooling rates from $dT/dt = -0.7$ to $-6$ K min$^{-1}$, where $t_0$ is found to monotonically decrease [e.g., by a factor of $\approx 4$ for $T = 411.8$ K (not shown)].

Most importantly, our fitting concept allows us to extrapolate the values of the initial susceptibility, $\chi_0(\omega) \equiv \chi'(\omega, \Delta t = -t_0) = \Delta\chi(\omega) + \chi_\infty(\omega)$, which are plotted in Fig. 3(b) versus $T$ for the above selected frequencies together with their inverse and "aged" values, $\chi_0^{-1}$ and $\chi_\infty$, respectively. As expected, the initial susceptibilities are much larger than the experimentally accessible ones [Fig. 1(b)]. They are peaking at an extrapolated transition temperature $T_0 \approx 411$ K with spectacularly large values, being largest for the lowest frequency, $\chi_0(37\ \text{Hz}, 411\ \text{K}) \approx 1.6 \times 10^6$, while decreasing by 99.2% to $\chi_\infty(411\ \text{K}) \approx 1.2 \times 10^4$ after ultimate aging. It is worth noting that the aged response becomes nearly frequency independent, while its peak shifts to higher temperatures, $\chi_\infty^{\max} \approx 4 \times 10^4$ at $T(\chi_\infty^{\max}) \approx 419$ K [Fig. 3(b)]. Its classical tail follows a Curie-Weiss-type behavior above 425 K and extrapolates a ferroelectric transition at $T_0 \approx 409.5$ K (not shown) in close coincidence with the initial Curie-Weiss behavior reflected by $(\chi')^{-1}(1\ \text{Hz})$ in Fig. 1(b).

The unaged response curve, which is in the focus of our interest, appears much narrower than the partially aged one. This is judged from comparing the inverse curves $(\chi')^{-1}(1\ \text{Hz})$ in Fig. 1(b) with $\chi_0^{-1}$ in Fig. 3(b), respectively, and numerically expressed by the exponent, $\gamma = 2.71 \pm 0.34$, emerging from a power-law fit within $412 \leq T \leq 419$ K for $\chi_0(f=37\ \text{Hz}) \propto (T-T_0)^{-\gamma}$ with $T_0 = 408.05 \pm 0.17$ K [Fig. 3(b); bold solid line]. As is well known, e.g., from the Landau theory of first-order transitions[21] a true divergence of $\chi_0$ is, indeed, expected at the lower bound $T_0$ of the hysteresis interval in zero external field ("Curie-Weiss temperature"). It can be considered a "first-order critical point" as introduced by Fisher and Berker,[22] where the order parameter undergoes

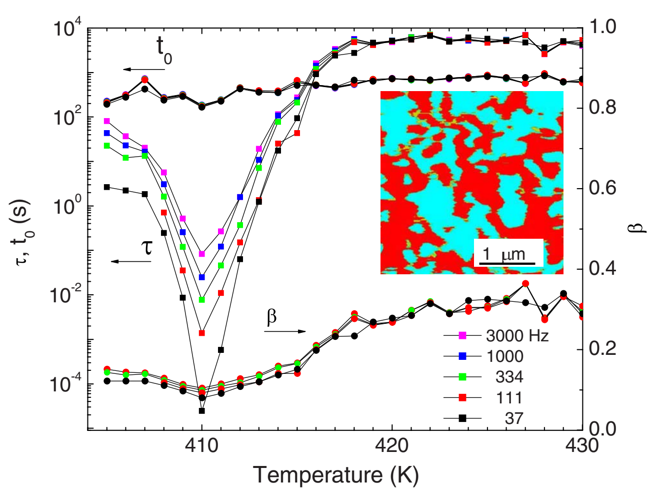


FIG. 4. (Color online) Parameters $\tau$, $t_0$, and $\beta$ (with lines to guide the eye) referring to best fits of Eq. (1) to all 130 aging curves $\chi$ vs $t$ [partially shown in Fig. 2(a)]. Inset: up/down/neutral (black/white/gray) domains imaged by PFM on the (001) face of a SBN40 crystal after aging for 1 year at room temperature (Ref. 12).

a discontinuity ($\delta \to \infty$), but the susceptibility diverges ($\gamma > 0$). The significance of the observed value of $\gamma$ is unclear. There are no theoretical predictions for the first-order RFIM scenario; but enhanced nonclassical values, $\gamma > 1$, are very likely. In the case of a second-order 3D RFIM transition one expects $\gamma = 1.7 \pm 0.2$,[23] in contrast to that of the 3D Ising model, $\gamma = 1.24$.[24]

We conclude that our system is expected to encounter a sharp first-order transition in its instantaneous state at $\Delta t = -t_0$, while rounding sets in after finite aging periods. For the ferroelectric system studied here, the system drops out of equilibrium quite far above $T_c$ by the formation of locally pinned polar regions. Owing to their own slow dynamics[13] an extrapolation to long times is the wrong way to obtain the equilibrium critical behavior. Hence, somewhat unexpectedly, instead of waiting very long times one has to extrapolate to short ones. The implication is that at times which are short on a scale of the experiment, but long compared to microscopic relaxation times, the system approaches the RFIM behavior. Quite sophisticatedly, these "short" times must still be longer than the exponentially divergent relaxation times of the RFIM.[5] Obviously, in the initially quenched paraelectric material droplets of the "wrong" ferroelectric phase evolve merely on the scale of the coherence length $\xi$ on approaching $T_0$ from above. This enables the phase transition to remain sharp[14] and to promote a percolating avalanche of the ferroelectric state[25] without being pinned by the network of metastable precursor domains of different polarities.

Only upon aging these are establishing above $T_0$ on a mesoscale by taking advantage of local fluctuations of the random fields and of the dipole-dipole interaction, where they have no chance to spread in a phase-transition manner. In any aged state these droplets are much larger than the polar correlation length $\xi$.[13,14] This initiates the severe rounding of the transition observed on usual time scales [Fig. 1(b)]. However, when coming sufficiently close to $T_0$ without aging, the correlation length $\xi$ has a chance to become larger than the droplets and thus to initiate an unsmeared phase transition.[14] Nevertheless, owing to activated critical slowing down in the presence of quenched random fields[5] a large dispersion is encountered in the ac susceptibility $\chi_0(T)$ as observed in Fig. 1(b). At the peak temperature (=apparent critical point), $T = 411$ K, a power law is found to be valid on a logarithmic frequency scale, $\chi_0(f, T = 411\text{ K}) = (1.1 \pm 0.2) \times 10^8 [\ln(f/\text{Hz})]^{-(1.54 \pm 0.11)}$, which is expected to convert at very low frequencies into the predicted asymptotic dynamic susceptibility $\lim_{\omega \to 0} \chi(\omega) \propto |\ln \omega|^{(2-\eta)/\theta}$, where $0 < 2 - \eta \leq \theta$.[5] Since our experiments are still far from the low-frequency limit, we are not able to extract reliable information on the exponents $\eta$ and $\theta$. Our investigation also leaves open the question of whether the observed first-order character of the transition in SBN40 might be due to a bimodal RF distribution, $\pm h$, as predicted by mean-field theory,[26] but ruled out for a Gaussian one.[7]

In conclusion, we have been able to reconstruct by temporal extrapolation the virgin state of the 3D random-field Ising model system $Sr_{0.40}Ba_{0.60}Nb_2O_6$, which undergoes a sharp weakly first-order phase transition on cooling at $T_0 = 411$ K. Thus, experimental access to the unaged state prior to the unavoidable aging by nanodomain formation[13] has become possible. In a next step we shall attempt to extend these experiments in order to study 3D RFIM criticality at a second-order phase transition. This will be possible by an evaluation of aging experiments at the electric critical point of SBN40, which occurs under a weak axial electric field, $E \approx 10$ kV/m, at $T_c \approx 415$ K.[27]

This work was supported by the Polish Ministry of Education and Science under Grant No. N507 455034. W.K. thanks the Foundation for Polish Science (FNP) for an Alexander von Humboldt Honorary Research Grant.

*Corresponding author; wolfgang.kleemann@uni-due.de


[1] J. P. Bouchaud *et al.*, in *Spin Glasses and Random Fields*, edited by A. P. Young (World Scientific, Singapore, 1997), p. 161.
[2] K. Fukao and S. Yamawaki, Phys. Rev. E **76**, 021507 (2007).
[3] K. Jonason *et al.*, Phys. Rev. Lett. **81**, 3243 (1998).
[4] Y. Imry and S. K. Ma, Phys. Rev. Lett. **35**, 1399 (1975).
[5] D. S. Fisher, Phys. Rev. Lett. **56**, 416 (1986).
[6] S. Fishman and A. Aharony, J. Phys. C **12**, L729 (1979).
[7] A. A. Middleton and D. S. Fisher, Phys. Rev. B **65**, 134411 (2002).
[8] F. Ye *et al.*, Phys. Rev. B **74**, 144431 (2006).
[9] W. Kleemann *et al.*, EPL **57**, 14 (2002).
[10] J. Dec *et al.*, Appl. Phys. Lett. **89**, 212901 (2006).
[11] W. Kleemann *et al.*, Phys. Rev. Lett. **97**, 065702 (2006); W. Kleemann, J. Phys.: Condens. Matter **18**, L523 (2006).
[12] V. V. Shvartsman *et al.*, Ferroelectrics **376**, 1 (2008).
[13] S. Semenovskaya and A. D. Khachaturyan, J. Appl. Phys. **83**, 5125 (1998).
[14] Y. Imry and M. Wortis, Phys. Rev. B **19**, 3580 (1979).
[15] T. Lukasiewicz *et al.*, J. Cryst. Growth **310**, 1464 (2008).
[16] S. Miga *et al.*, Rev. Sci. Instrum. **78**, 033902 (2007).
[17] The Curie-Weiss temperature $T_0$ designates the thermodynamic lower bound of the thermal hysteresis of the first-order phase transition in zero electric field. The upper bound and the equilibrium transition temperature are located at $T_1$ and $T_c$, respectively, where $T_0 < T_c < T_1$.
[18] S. Miga *et al.*, Phys. Rev. B **70**, 134108 (2004).
[19] F. Alberici *et al.*, J. Phys. I **7**, 329 (1997); O. Kircher and R. Böhmer, Eur. Phys. J. B **26**, 329 (2002).
[20] K. Binder and J. D. Reger, Adv. Phys. **41**, 547 (1992).
[21] J. C. Tolédano and P. Tolédano, *The Landau Theory of Phase Transitions* (World Scientific, Singapore, 1987).
[22] M. E. Fisher and A. N. Berker, Phys. Rev. B **26**, 2507 (1982).
[23] H. Rieger, Phys. Rev. B **52**, 6659 (1995).
[24] J. C. Le Guillou and J. Zinn-Justin, Phys. Rev. Lett. **39**, 95 (1977).
[25] J. P. Sethna *et al.*, Phys. Rev. Lett. **70**, 3347 (1993).
[26] A. Aharony, Phys. Rev. B **18**, 3318 (1978).
[27] J. Dec, S. Miga, and W. Kleemann (unpublished).